Journal of Luminescence 129 (2009) 996–999

Contents lists available at ScienceDirect

Journal of Luminescence

journal homepage: www.elsevier.com/locate/jlumin

Abnormal blueshift of UV emission in single-crystalline ZnO nanowires

Dandan Wang [a,b], Jinghai Yang [c,a,b,*], Guozhong Xing [d,e], Lili Yang [c], Jihui Lang [c], Ming Gao [c], Bin Yao [a,d], Tom Wu [e]

[a] Key Laboratory of Excited State Processes, Changchun Institute of Optics, Fine Mechanics and Physics, Chinese Academy of Sciences, Changchun 130033, China
[b] Graduate School of the Chinese Academy of Sciences, Beijing 100049, China
[c] Institute of Condensed Matter Physics, Jilin Normal University, Siping 136000, China
[d] Department of Physics, Jilin University, Changchun 130023, China
[e] Division of Physics and Applied Physics, School of Physical and Mathematical Sciences, Nanyang Technological University, Singapore 637371, Singapore

ARTICLE INFO

Article history:
Received 14 January 2008
Received in revised form
16 March 2009
Accepted 9 April 2009
Available online 18 April 2009

PACS:
78.55.Et
81.10.Bk
81.05.Dz

Keywords:
ZnO
Nanostructure
Crystal growth
Optical property
Blueshift

ABSTRACT

Single-crystalline ZnO nanowires (NWs) were synthesized by a facile vapor transport method. The good orientation and high crystal quality were characterized by X-ray diffraction (XRD), scanning electron microscope (SEM) and high-resolution transmission electron microscope (HRTEM) measurements. Excitation-power-dependence photoluminescence spectra of ZnO NWs show that the UV emission displayed an evident blueshift with increasing excitation power and the corresponding energy shift might be as large as 10 meV. This anomalous phenomenon correlates to the band bending level caused by the surface built-in electric field due to the existence of substantial oxygen vacancies. By increasing the excitation power, the enhanced neutralization effect near the surface will reduce the built-in electric field and lead to a reduction of band bending which triggers the blueshift of the UV emission.

© 2009 Elsevier B.V. All rights reserved.

1. Introduction

One-dimensional nanostructures, such as nanowires (NWs), nanorods, nanobelts and nanotubes have become the focus of intensive research due to their unique applications in microscopic physics and fabrication of nanoscaled devices [1–6]. With a wide bandgap (3.37 eV) and large exciton binding energy (60 meV) at room temperature, zinc oxide (ZnO), an exceptionally important semiconductor, has attracted extensive attention as a prime candidate for nanoscale optoelectronics applications such as photodetectors [7], light-emitting diodes [8] and lasers [9]. A good optoelectric device should not only have high luminous efficiency, high thermostability and low threshold of luminescence, but also can be tuned effectively and easily. Intrinsic ZnO NWs have been observed to emit radiation in the UV and visible spectral region at room temperature. The visible emission of ZnO is usually ascribed to structural defects [10–12]. The UV emission is attributed to the near-band-edge emission, and arises from the recombination of free excitons through an exciton–exciton collision process [13,14]. Many works focus on increasing UV emission and restraining visible emission. However, how to adjust UV emission location also plays a significant role in the optoelectronic application of ZnO nanostructures. Until now, although the UV emission location can be well adjusted through changing the diameter of ZnO nanostructures into quantum scope [15], it is relatively difficult to fabricate such small size and control the size exactly. On the contrary, using external conditions to control the UV emission location should be an easier way [16–19]. Our work is mainly focused on excitation-power-dependent photoluminescence (PL) characterization. The results show that by increasing the excitation power, the UV emission exhibits an obvious blueshift. Although there are some ways such as doping [20] that can adjust the UV emission, this easy method via adjusting external light beam to manipulate the photoluminescence characteristics should pave an insight for the research on adjustable optoelectronic devices, and this method can also be extended to the study of other nanoscaled semiconductors.

* Corresponding author at: Key Laboratory of Excited State Processes, Changchun Institute of Optics, Fine Mechanics and Physics, Chinese Academy of Sciences, Changchun 130033, China. Tel.: +86 434 3290009.
E-mail address: jhyang@jlnu.edu.cn (J. Yang).

0022-2313/$ - see front matter © 2009 Elsevier B.V. All rights reserved.
doi:10.1016/j.jlumin.2009.04.012

2. Experiments

A mixture of ZnO powder (99.99%, 325 mesh, Alfa Aesar) and graphite powder (99.99%, 325 mesh, Alfa Aesar) with a weight ratio of 1:1 were ground 50 min before being placed in an alumina boat covered with the Au-coated Si substrates. The alumina boat was inserted into a small quartz tube. When the initial temperature of the furnace was heated up to 850 °C, the small quartz tube was put into the furnace as shown in Fig. 1. With the Ar gas flowing into the furnace, the temperature was immediately ramped to 900 °C and then cooled down quickly to room temperature after being kept at 900 °C for an hour. After the reaction, a layer of white product was found on the Si substrates. Then Si substrate with white product sample was cut into two pieces, one is named as the as-grown sample; another was annealed at 600 °C for one hour in air which is named as annealed sample. The morphology of products was characterized by using a scanning electron microscope (SEM, Hitachi S-570). The crystal structure of the NWs was determined using X-ray diffraction (XRD, MAC Science, MXP18) and high-resolution transmission electron microscope (HRTEM, JEOL JEM-2010). The chemical compositions were examined by X-ray photoelectron spectroscopy (XPS, VG ESCALAB MKII system equipped with a monochromatic X-ray source), the data analysis was done using XPSPEAK 4.1 software (UK Surface Analysis). Photoluminescence was performed at room temperature by using a Jobin Yvon T64000 system with a He–Cd laser at a wavelength of 325 nm. The samples were mounted on a *xyz*-table which moves the samples to the intersection point of the laser beam and the optical axis to achieve better signal to noise ratio. The signals were collected with Olympus camera lens. Multiple curves were recorded to ensure the data reproducibility.

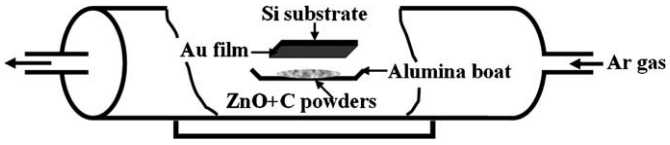

Fig. 1. Schematic illustration of ZnO NWs growth setup.

3. Results and discussions

Fig. 2(a) shows an SEM image of the as-grown ZnO NWs with diameter of ~180 nm over a large area. Inset is the magnified top view of single NW. It can be clearly seen that the top of the NWs has very smooth surface with hexagonal shape. The TEM image (Fig. 2(b)) of individual NW indicates that the synthesized ZnO NWs have smooth surface, which is well consistent with the SEM observations. The inset SAED pattern confirms that the nanowire grows along the *c*-axis direction, which is also consistent with the XRD results. No splitting of the diffraction spots was observed. Fig. 2(c) shows the HRTEM image of ZnO NWs. The image clearly reveals the lattice fringes with the distance between two lattice fringes of about 0.521 nm, corresponding to the ZnO (0 0 1) fringe, which is consistent with that of a bulk wurtzite ZnO crystal. The HRTEM observations confirms that the grown NWs are single crystalline with the wurtzite hexagonal phase and that they grow along the [0 0 1] direction.

X-ray diffraction pattern of the as-grown nanowires is indexed as a hexagonal wurtzite ZnO structure as shown in Fig. 2(d). The dominating diffraction peak of ZnO (0 0 2) appears obviously in the patterns. There are also diffraction peaks of ZnO (1 0 0), ZnO (1 0 1) and ZnO (1 0 3), but the intensity of these peaks is very weak, which indicates that the ZnO NWs are preferentially oriented in the *c*-axis direction. Moreover, no diffraction peaks from Zn or other impurities are observed within the detect limitation.

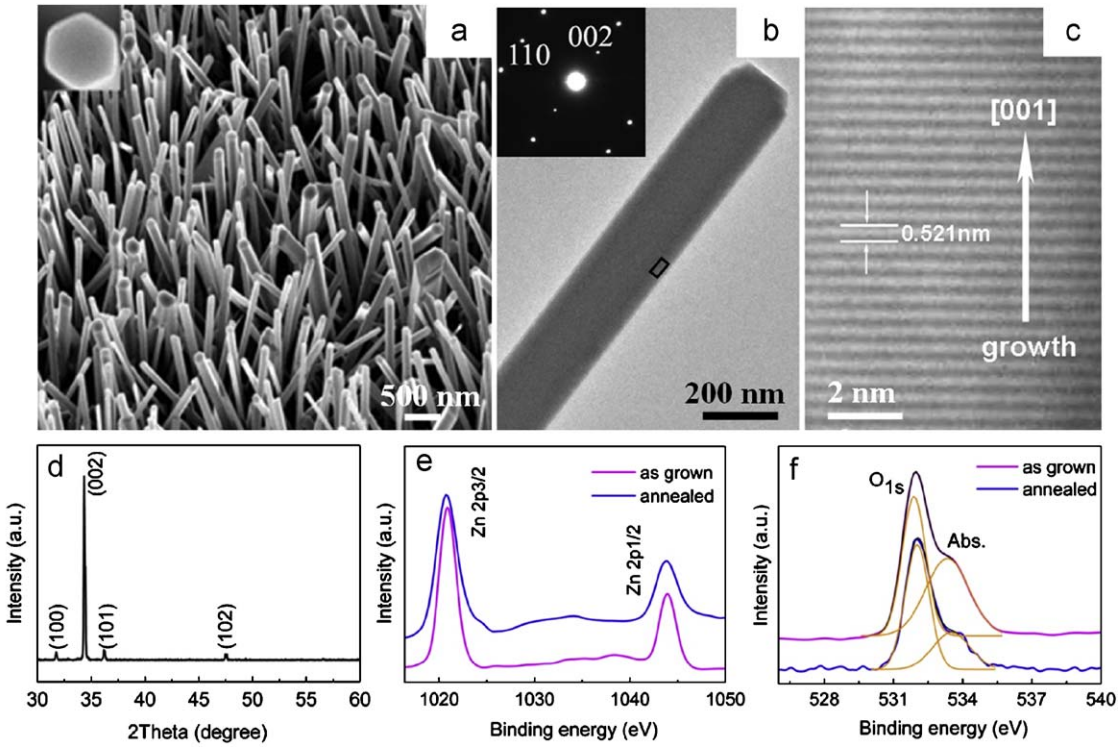

Fig. 2. (color online) (a) SEM image of the as-grown ZnO NWs over a large area. (b) TEM image of the as-grown single NW. Inset is the corresponding SAED pattern. (c) HRTEM image of an individual NW, corresponding to the area enclosed by the dashed lines in (b). (d) XRD patterns of ZnO NWs. X-ray photoelectron spectroscopy detail scans of the as-grown and after annealing ZnO NWs: (e) Zn_{2p} and (f) O_{1s} core-level spectra.

To further investigate the chemical compositions and valence states, XPS measurements were performed on the nanowires samples. Fig. 2(e, f) shows XPS spectra taken from the Zn and O regions of the as-grown ZnO NWs and annealed ZnO NWs. The peaks at 1020.9 and 1043.9 eV (Fig. 2(e)) are due to the binding energy of $Zn_{2p3/2}$ and $Zn_{2p1/2}$, respectively. In Fig. 2(f), we can see that the O_{1s} profile is asymmetric. It was fitted by using Gaussian functions which gave better deconvolutions. Two Gaussian curves were extracted for the spectrum, and two peaks are located at 531.8 and 533.3 eV, respectively. The peak at about 531.8 eV attributed to the O^{2-} ions in the wurtzite structure, whereas the weaker shoulder peak at about 533.3 eV is due to chemisorbed oxygen caused by surface hydroxyl, which corresponds to O–H bonds [21]. No peaks of other impurities were observed within the detection limit. The atomic composition of Zn and O (excluding OH) were calculated by using the integrated peak area and atomic sensitivity factors, and the relative oxygen content of the as-grown ZnO NWs and annealed ZnO NWs were 45.2% and 48.1%, implying that there exist substantial oxygen vacancies in the ZnO NWs, but after annealing in the air it decreased significantly.

Fig. 3 shows the room-temperature excitation-power-dependent PL spectra of the as-grown ZnO NWs (Fig. 3(a)) and annealed ZnO NWs (Fig. 3(b)). It can be observed that the UV emission intensity of two samples increased with increasing excitation power, consistent with previous report [22]. However, the UV emission displayed an evident blueshift both for the as-grown ZnO NWs and annealed ZnO NWs, and the inset of Fig. 3(a, b) shows that the increase in the peak energy of the as-grown ZnO NWs could be as large as 10 meV, but only 2.2 meV for the annealed ZnO NWs. We also observed the same trend on the as-grown ZnO nanobelts, nanoneedles, nanodumbbells and corresponding annealed samples, respectively (not show here). Lieber and Wang groups also observed a blueshift of lasing peaks in InGaN multi-quantum-well nanowire, which was due to the band filling and/or photo-induced screening of internal electric fields [19]. But Szarko and Song et al. reported a redshift of the band-edge emission for the nanowire and nanotetrapod, which due to the bandgap renormalization resulted from the screening of the coulomb interaction and exchange and correlation effects [16–18]. In our measurement, due to the low excitation intensity, the bandgap renormalization resulting from the electron–hole plasma (EHP) emission built with a cooling process from hot carriers to a quasi-thermalized system was not significant. ZnO NWs exhibit intrinsic high surface-to-volume ratio, and from the XPS analysis, they possess substantial oxygen vacancies, which give rise to the possibility that the electron can be trapped, thereby creating a surface built-in electric field. Synchronously, the oxygen vacancies extract electrons from the conduction band of ZnO and form a depletion layer on the surface [23–25], which results in an upward band bending near the surface, as shown in Fig. 3(c). Consequently the upward band bending will reduce the bandgap energy. Under optical excitation, more photoexcited electrons and holes separated and swept in opposite directions by the built-in electric field. Negatively charged states will neutralize more holes, which are attracted to the surface. The enhanced neutralization effect will reduce the built-in electric field and lead to a reduction of the band bending [26], and then finally increase the transition energy of the exciton. The shift of the excitation-power-dependent Raman scattering spectra (not shown here) also confirm that the change of the build-in electric field with different optical excitation, which is due to the converse piezoelectric effect of ZnO. After the annealing treatment, the crystal quality is undoubtedly improved. This is confirmed by the XPS results which show that the oxygen vacancies concentration is 2.9% smaller than the as-grown ZnO NWs. The level of the upward band bending result from depletion layer is lower than that of the as-grown ZnO NWs. So under optical excitation, the blueshift of band-edge emission of the annealed ZnO NWs is smaller than that of the as-grown ZnO NWs.

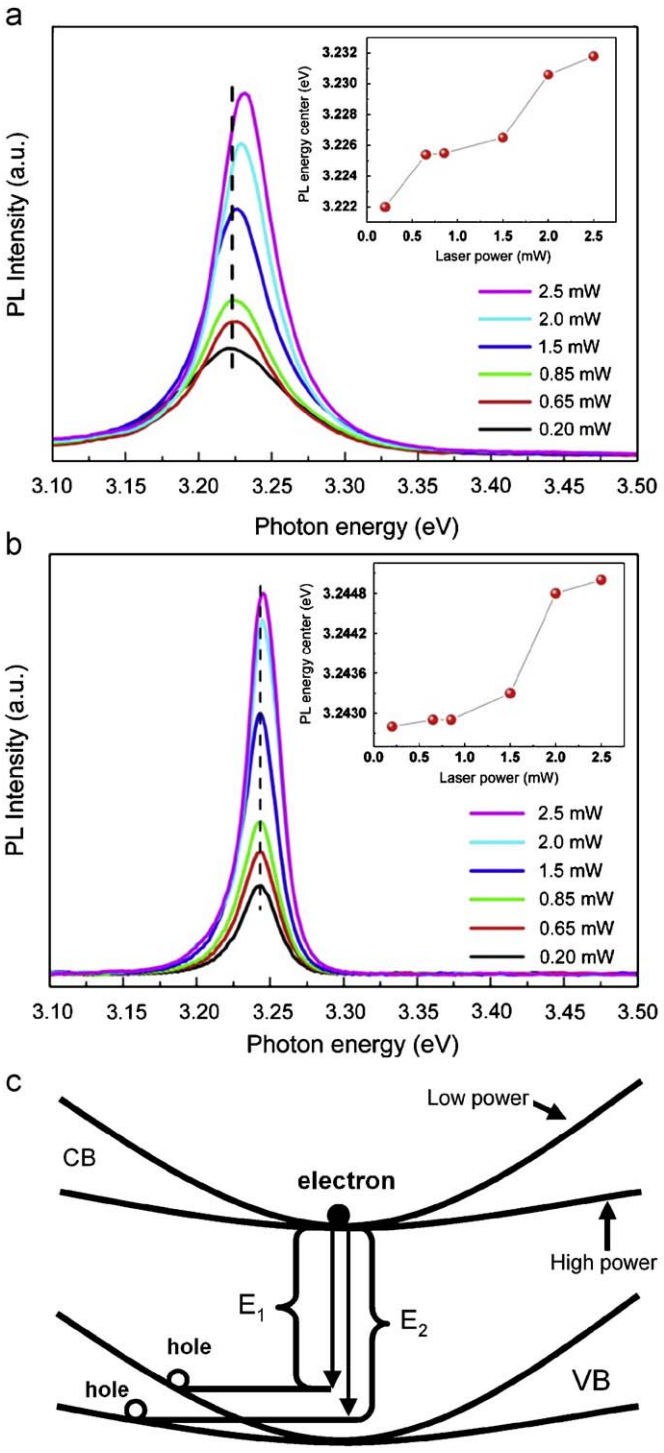

Fig. 3. (color online) Excitation power dependence of the photoluminescence spectra of as-grown ZnO NWs (a) and annealed ZnO NWs (b). The inset pattern is the PL peak energy under different excitation power. (c) Schematic illustration of band energy under low and high excitation power.

4. Conclusion

In summary, single-crystalline ZnO NWs with good crystal orientation were synthesized via the facile vapor transport method. With increasing excitation power, the UV peaks move toward the high-energy region. After being annealed in air, the blueshift becomes smaller. We believe that the blueshift of the PL spectra can be attributed to a reduction in the level of band bending caused by illumination. Our results provide a useful insight for application of optoelectric devices based on ZnO NWs.

Acknowledgements

This work was supported by the program of the National Natural Science Foundation of China (Nos. 60778040 and 60878039), gifted youth program of Jilin province (No. 20070118), the Key Project for Science and Technology of Chinese Ministry of Education (Item no. 207025), the program for importing foreign technology and management talents into China (Item no. S20072200001), the Eleventh Five-Year Program for Science and Technology of Education Department of Jilin Province (Item nos. 20070162, 20070149, 20080154 and 20080156) and Program for the development of Science and Technology of Jilin province (Item no. 20070707).

References

[1] Z.L. Wang, J. Phys. Condens. Mater. 16 (2004) 829.
[2] M.H. Huang, S. Mao, H. Feick, H. Yan, Y. Wu, H. Kind, E. Weber, R. Russo, P. Yang, Science 292 (2001) 1897.
[3] G.Z. Xing, J.B. Yi, J.G. Tao, T. Liu, L.M. Wong, Z. Zhang, G.P. Li, S.J. Wang, J. Ding, T.C. Sum, C.H.A. Huan, T. Wu, Adv. Mater. 20 (2008) 3521.
[4] Z. Zhang, Y.H. Sun, Y.G. Zhao, G.P. Li, T. Wu, Appl. Phys. Lett. 92 (2008) 103113.
[5] S.C. Minne, S.R. Manalis, C.F. Quate, Appl. Phys. Lett. 67 (1995) 3918.
[6] Z. Zhang, S.J. Wang, T. Yu, T. Wu, J. Phys. Chem. C 111 (2007) 17500.
[7] H. Kind, H. Yan, B. Messer, M. Law, P. Yang, Adv. Mater. 14 (2002) 158.
[8] C.H. Liu, J.A. Zapien, Y. Yao, X.M. Meng, C.S. Lee, S.S. Fan, Y. Lifshitz, S.T. Lee, Adv. Mater. 15 (2003) 838.
[9] P. Yang, H. Yan, S. Mao, R. Russo, J. Johnson, R. Saykally, N. Morris, J. Pham, R. He, H.J. Choi, Adv. Funct. Mater. 12 (2002) 323.
[10] J.H. Yang, J.H. Lang, L.L. Yang, Y.J. Zhang, D.D. Wang, H.G. Fan, H.L. Liu, Y.X. Wang, M. Gao, J. Alloys Compd. 450 (2008) 521.
[11] C.C. Tang, S.S. Fan, M.L. Chapelle, P. Li, Chem. Phys. Lett. 333 (2001) 12.
[12] D.D. Wang, J.H. Yang, L.L. Yang, Y.J. Zhang, J.H. Lang, M. Gao, Cryst. Res. Technol. 43 (2008) 1041.
[13] Y.C. Kong, D.P. Yu, B. Zhang, W. Fang, S.Q. Feng, Appl. Phys. Lett. 78 (2001) 407.
[14] J.H. Yang, D.D. Wang, L.L. Yang, Y.J. Zhang, G.Z. Xing, J.H. Lang, H.G. Fan, M. Gao, Y.X. Wang, J. Alloys Compd. 450 (2008) 508.
[15] D. Sun, H.J. Sue, N. Miyatake, Appl. Phys. Lett. 112 (2008) 16002.
[16] J.M. Szarko, J.K. Song, C.W. Blackledge, I. Swart, S.R. Leone, S. Li, Y. Zhao, Chem. Phys. Lett. 404 (2005) 171.
[17] J.K. Song, J.M. Szarko, S.R. Leone, S. Li, Y. Zhao, J. Phys. Chem. B 109 (2005) 15749.
[18] J.K. Song, U. Willer, J.M. Szarko, S.R. Leone, S. Li, Y. Zhao, J. Phys. Chem. C 112 (2008) 1679.
[19] F. Qian, Y. Li, Grade, S. ccaron, Nat. Mater. 7 (2008) 701.
[20] L.M. John, H. Jesse, H. Heather, C. Erin, M. James, B. Leah, M.G. Norton, J. Appl. Phys. 104 (2008) 123519.
[21] M. Futsuhara, K. Yoshioka, O. Takai, Thin Solid Films 317 (1998) 322.
[22] S.C. Lyu, Y. Zhang, H. Ruh, H.J. Lee, H.W. Shim, E.K. Suh, C.J. Lee, Chem. Phys. Lett. 363 (2002) 134.
[23] T. Gao, T.H. Wang, Appl. Phys. A 80 (2005) 1451.
[24] J. Chunming, T. Ashutosh, J.N. Roger, J. Appl. Phys. 98 (2005) 083707.
[25] X.L. Wu, G.G. Siu, C.L. Fu, H.C. Ong, Appl. Phys. Lett. 78 (2001) 2285.
[26] K. Vanheusden, W.L. Warren, C.H. Seager, D.R. Tallant, J.A. Voigt, B.E. Gnade, J. Appl. Phys. 79 (1996) 7983.